Smart Driving of a Vehicle Using Model Predictive Control for Improving Traffic Flow

Md. Abdus Samad Kamal, *Member, IEEE*, Jun-ichi Imura, *Member, IEEE*, Tomohisa Hayakawa, *Member, IEEE*, Akira Ohata, and Kazuyuki Aihara

***Abstract*—Traffic management on road networks is an emerging research field in control engineering due to the strong demand to alleviate traffic congestion in urban areas. Interaction among vehicles frequently causes congestion as well as bottlenecks in road capacity. In dense traffic, waves of traffic density propagate backward as drivers try to keep safe distances through frequent acceleration and deceleration. This paper presents a vehicle driving system in a model predictive control framework that effectively improves traffic flow. The vehicle driving system regulates safe intervehicle distance under the bounded driving torque condition by predicting the preceding traffic. It also focuses on alleviating the effect of braking on the vehicles that follow, which helps jamming waves attenuate to in the traffic. The proposed vehicle driving system has been evaluated through numerical simulation in dense traffic.**

***Index Terms*— Automotive control, connected vehicles environment, model predictive control (MPC), traffic congestion.**

I. Introduction

TRAFFIC congestion on road networks is one of the most significant problems that is faced in almost all urban areas. Traffic congestion wastes time and produces pollutant exhaust-gas emissions in the atmosphere. Driving under traffic congestion compels frequent idling, acceleration, and braking, which increase energy consumption and wear and tear on vehicles. When the number of vehicles increases beyond the road capacity and the traffic density exceeds a certain value, free-flow traffic turns into congested traffic. Such traffic jams are common in the morning and afternoon rushes, when a large number of vehicles successively enter into the road network. This type of jam can be alleviated either by restricting the number of vehicles in the congested area or by increasing the road capacity.

Traffic congestion may also occur due to complex interactions among vehicles and due to the influences of some incidents that disturb the traffic flow in medium to high traffic density [1]. In other words, such congestion depends on how the drivers follow other vehicles in dense traffic. Aggressive drivers, who drive very quickly with high acceleration in short distances, or slow drivers often disturb traffic flow. Such disturbances in dense traffic originate density waves that propagate backward by increasing the magnitude and that ultimately form shock waves or traffic breakdown. Traffic jams that appear in the absence of bottlenecks or with no apparent reasons are termed as "phantom traffic jams" in [2] and they are experimentally observed in [3]. Often, this type of traffic jam contain self-sustaining traffic density waves, which are termed as "Jamitons" in [4]. It is expected that the occurrence of such traffic jams due to poor *ad hoc* driving can be prevented or at least alleviated by proper control of vehicles and coordination of traffic.

Some studies show that the occurrence of such shock waves or traffic breakdown can be prevented by imposing a speed limit [5]. A model predictive control (MPC) approach was presented to optimally adjust variable speed limits for freeway traffic, with the aim of suppressing shock waves [6]. By efficiently maneuvering vehicles, traffic flow can be improved. An adaptive cruise control (ACC) system in a car automatically detects its leading vehicle and adjusts the headway (intervehicle distance) by using both the throttle and the brake. Conventional ACC systems offer better comfort and safety in favorable driving situations [7], but they are not suitable in congested traffic conditions due to their response delay. An ACC system with negligible response time can be effective in improving traffic flow. It was demonstrated that, if 25% of vehicles in highway traffic were equipped with ACC systems, congestion would be completely avoided [8].

Some advanced ACC systems, such as the cooperative ACC (CACC), receive the driving information from the preceding vehicle (PV) through a communication network with very little time delay and have a much shorter response time than human drivers [8], [9]. A quick responding ability makes the CACC string stable, i.e., any disturbances, braking effects, or congestion-forming phenomena are attenuated over time [10], [11]. In addition, CACC systems can safely drive vehicles with very short headway by forming a platoon that also increases the traffic capacity of the road network.

Manuscript received April 11, 2013; revised September 9, 2013; accepted November 13, 2013. Date of publication January 2, 2014; date of current version March 28, 2014. This work was supported in part by the Aihara Innovative Mathematical Modeling Project and in part by the Japan Society for the Promotion of Science through the Funding Program for World-Leading Innovative Research and Development on Science and Technology (FIRST Program), which is initiated by the Council for Science and Technology Policy. The Associate Editor for this paper was L. Li.

M. A. S. Kamal is with the Japan Science and Technology Agency, Kawaguchi 332-0012, Japan, and also with the Institute of Industrial Science, The University of Tokyo, Tokyo 153-8505, Japan (e-mail: maskamal@ieee.org).

J. Imura and T. Hayakawa are with the Department of Mechanical and Environmental Informatics, Graduate School of Information Science and Engineering, Tokyo Institute of Technology, Tokyo 152-8552, Japan.

A. Ohata is with the Toyota Motor Corporation, Shizuoka 410-1193, Japan.

K. Aihara is with the Collaborative Research Center for Innovative Mathematical Modelling, Institute of Industrial Science, The University of Tokyo, Tokyo 153-8505, Japan, and also with the Graduate School of Information Science and Technology, The University of Tokyo, Tokyo 113-8656, Japan.

Color versions of one or more of the figures in this paper are available online at http://ieeexplore.ieee.org.

Digital Object Identifier 10.1109/TITS.2013.2292500

Most ACC systems use the information of the immediate PV and generate control action without anticipating future traffic situations. In contrast, human drivers perceive the traffic situation with several vehicles ahead and are often able to take anticipated driving action in advance. An advanced ACC system that uses the information of several vehicles in the surrounding traffic and that adopts sophisticated predictive control is expected to be more efficient. The connected vehicles environment would make it possible to realize such vehicle control systems. The connected vehicles environment provides a two-way wireless communication environment that enables vehicle-to-vehicle (V2V) and vehicle-to-infrastructure (V2I) communications [12], [13]. In the connected vehicles environment, precise information of the local traffic can be easily obtained with negligible delay and accurate prediction of the local traffic flow can be performed.

Recently, we have presented a vehicle control framework to drive a vehicle efficiently [14]. In this framework, a single vehicle, which is called the host vehicle, is driven by predicting its few PVs using the MPC. Therefore, it differs from the conventional CACCs in the sense that they control multiple vehicles in a platoon without any prediction of their future situations. The main point of the framework is to only regulate the host vehicle by adjusting its safe headway without an aggressive control action. It was found that the host vehicle avoided aggressive braking and large speed drops in spite of the jamming waves in the preceding traffic. Although the dynamics of the following vehicles (FVs) were not considered in determining the control action, the predictive control that was applied to the host vehicle also improved the behavior of other vehicles in the following traffic when information from a sufficiently large number of PVs is obtained (see [14] for further details). Consequently, it is understood that considering the dynamic behavior of the FV in the host-vehicle control framework may smooth the traffic flow more effectively.

By enhancing the vehicle control framework, in this paper, a smart-driving system using the MPC is proposed, which focuses on more effectively smoothing the traffic flow by controlling a vehicle. Here, human-driven traffic is assumed to be imitated by a microscopic traffic-flow model known as the optimal velocity model (OVM) [15]. The OVM is used for both predicting the traffic in the MPC framework and evaluating the effectiveness of the proposed smart-driving system through numerical simulation. In this formulation, the dynamic behavior of the FV is included in the host-vehicle control model. Such inclusion is natural and helpful in avoiding sudden braking in the FV or avoiding a rear-end collision when it follows the host vehicle closely, although the FV is driven independently. The control framework explicitly considers the dynamics of a few PVs and predicts the future trajectory of the immediate PV. Using the predicted trajectories of the PV, at each short time interval the smart-driving system computes the control input for the host vehicle using the MPC and regulates its safe headway. The performance index of the MPC includes the costs of acceleration in both the host and the FVs, which enables the smart-driving system to control the host vehicle such that the accelerations of both vehicles are sufficiently gentle. Consequently, any waves of traffic density are effectively attenuated in the following traffic.

The performance of the proposed control framework is evaluated on uniformly distributed dense traffic through numerical simulation. For simplicity, in this paper, the computed optimal control input (in the context of the MPC) is directly fed to drive the host vehicle, assuming that the advanced ACC system requests the torque, and the engine exactly follows it without any delay. It is found that the host vehicle that is controlled by the smart-driving system significantly reduces the velocity fluctuations and the FVs also benefit as their flowing behavior is improved significantly.

The rest of this paper is organized as follows. Section II describes a traffic-flow model and the formation of jamming waves at high traffic density. The vehicle control framework, along with the problem formulation, assumptions, prediction models, and an algorithm using nonlinear MPC, is presented in Section III. Section IV describes the simulation setting and results. Section V discusses some aspects of the proposed system. Finally, Section VI concludes this paper. In addition, a brief overview of the continuation and generalized minimal residual method used for solving the MPC problem is described in the Appendix.

II. Propagation of Jamming Waves

Research related to the modeling behavior of human-driven vehicular traffic and traffic congestion in various conceptual frameworks has a long track record [1], [16]. For later convenience, a microscopic traffic-flow model is briefly described in this section, which is followed by an illustration of how jamming waves evolve on a straight road without any physical obstructions. Specifically, the OVM is chosen in this paper for its computational simplicity as a microscopic traffic-flow model. The OVM simply represents human driving behavior by a differential equation with a few parameters, and it describes many properties of real traffic flow [15]. The OVM is formulated based on the presumption that a car is driven to reach a velocity depending on the headway in a short interval of time and this velocity is conventionally called the optimal velocity. The expression of the acceleration of a vehicle in the OVM is given by

$$\ddot{x}_n = \kappa \left[V_{\mathrm{op}}(\Delta x_n) - \dot{x}_n \right] \tag{1}$$

where n is the index number of the vehicle, x_n is its position, $\Delta x_n = x_{n-1} - x_n$ is the headway (the range clearance from the PV $n-1$), $V_{\mathrm{op}}(\Delta x_n)$ denotes the optimal velocity as a function of the headway defined by (3), and κ is the sensitivity. The sensitivity is the inverse of the delay time that is required to reach the optimal velocity.

The stability of the OVM was studied for both the periodic [1], [15] and open boundary conditions [17] of a traffic flow. These studies revealed that the traffic flow that is represented by the OVM is locally string stable, depending on the density of the traffic. If the traffic density is higher than the critical traffic density, the traffic flow may become unstable due to fluctuations

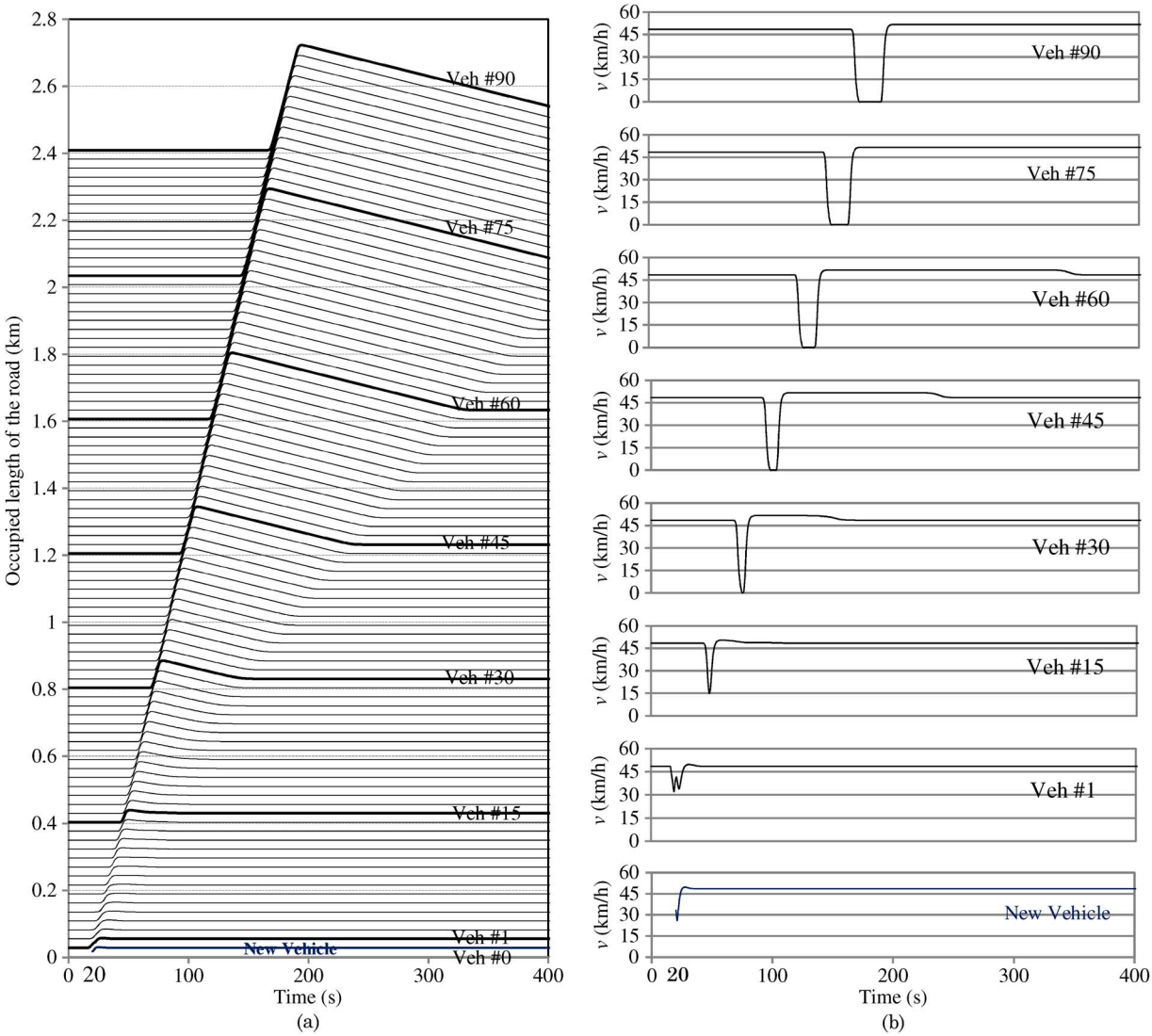

Fig. 1. Spontaneous formation of a jamming wave due to the appearance of a new vehicle in front of the first vehicle in highly dense traffic. (a) Relative positions of the vehicles to Veh #0; the gap between two curves shows the corresponding distance of two vehicles. (b) Corresponding velocities (v, km/h) of selected vehicles in the traffic.

in any vehicle. The critical headway h that is associated with the critical traffic density is related by the neutral stability condition

$$V'_{\rm op}(h) = \frac{\kappa}{2} \tag{2}$$

where $V'_{\rm op}(h)$ is the derivative of optimal velocity $V_{\rm op}(\Delta x)$ at $\Delta x = h$. Under the condition that $V'_{\rm op}(h) > \kappa/2$, small disturbances (fluctuation or deviation from the uniform steady flow) in any vehicle amplify in time and propagate over the FVs; uniform traffic changes into a different dynamical state, and the vehicle string becomes unstable. On the other hand, for $V'_{\rm op}(h) \leq \kappa/2$, any small disturbance decays in time and the vehicle string remains stable. This string-stability condition is valid for any optimal velocity function $V_{\rm op}(\cdot)$ [1].

Various representations of $V_{\rm op}(\cdot)$ using a hyperbolic tangent function have been proposed [15], [18]–[20]. In this paper, for the purpose of using (1), the velocity function proposed by Helbing and Tilch [18] is chosen, which has the form

$$V_{\rm op}(\Delta x_n) = V_1 + V_2 \tanh\left[C_1(\Delta x_n - {\rm l}_c) - C_2\right] \tag{3}$$

where l_c is the minimum allowable distance from the PV, including its length at zero velocity. In [18], the parameters of (1) and (3) are approximated through the calibration of the OVM with respect to the empirical follow-the-leader data for city traffic with a limited maximum velocity, which are $\kappa = 0.85\ {\rm s}^{-1}$, $V_1 = 6.75$ m/s, $V_2 = 7.91$ m/s, $C_1 = 0.13\ {\rm m}^{-1}$, and $C_2 = 1.57$. With these parameters of the optimal velocity function, a critical headway of $h \simeq 24.85$ m is obtained from (2), which corresponds to a critical traffic density of approximately 40.25 vehicles per kilometer (veh/km).

Fig. 1 illustrates the phenomena that correspond to the dynamic evolution of traffic density waves in dense human-driven vehicular traffic. This simulation is conducted using identical vehicles that are driven according to (1) and (3) on a straight flat road, where the minimum separation between vehicles, including the car length $l_c = 5$ m, is taken into account. Initially, at time $t = 0$ s, all vehicles are running with an equal separation of $\Delta x = 26.75$ m and an optimal velocity of $V_{\rm op}\ (26.75) = 13.47$ m/s. The flowing behavior of vehicles, which is marked by Veh #0–Veh #90, are shown in the figure. At $t = 20$ s, a

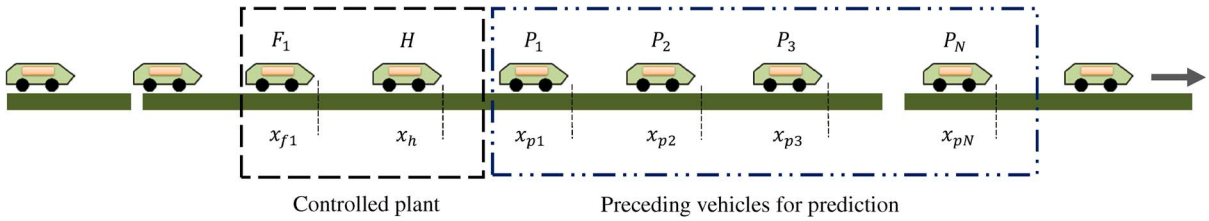

Fig. 2. Vehicle control problem for controlling a host vehicle (H), considering its immediate PV P_1 and immediate FV F_1. Jamming waves are predicted using the dynamics of vehicles P_1 to P_N.

new vehicle from another lane or an external road suddenly enters into the traffic in between vehicles Veh #0 and Veh #1. Therefore, the headway of the first vehicle (Veh #1) largely shrinks and, consequently, its velocity is reduced to safely accommodate the new vehicle in the traffic. Vehicle Veh #0 remains unaffected by the new vehicle and continues cruising at its initial velocity. The first vehicle almost reclaims its steady velocity in the next 13 s and continues running steadily.

However, the fluctuation of the headway or velocity increases in the second vehicle, and it propagates backward by increasing the magnitude and the duration. Such transitory fluctuations of the headway in the successive vehicles create a density wave in the traffic, which is shown in Fig. 1 and is henceforth referred to as a jamming wave in this paper. The curves in Fig. 1(a) represent the relative positions of the vehicles to Veh #0. The gap between two consecutive curves represents the corresponding headway. At $t = 0$ s and at around $t = 100$ s, these vehicles are distributed in 2.38 km on the road, with an average density of 37.38 veh/km. However, due to the propagation of the jamming wave at about $t = 195$ s, these vehicles occupy a space of about 2.67 km on the road.

The corresponding velocities of some selected vehicles are shown in Fig. 1(b). The 30th vehicle and the others behind it have to come to a complete stop for a while to keep their clearances safe due to the influence of the jamming waves. The 90th vehicle is affected by the jamming wave for the duration of $t = 197$ s to $t = 559$ s (the curve for $t > 400$ s is not shown in the graph) and it has to completely stop for about 19 s.

At the initial operating point $\Delta x = 26.75$ m, the vehicles were string stable according to condition (2), since $V'_{\rm op}\ (26.75) = 0.284$, which is much less than $\kappa/2 = 0.425$. However, a large deviation that is due to the new vehicle causes a drop in the headway of some local vehicles, and they seem to fall under the condition that $V'_{\rm op}(h) > \kappa/2$ and become unstable. A close look at the jamming wave in Fig. 1 hints at the way of avoiding such fluctuations technically. For example, at about $t = 100$ s, if the 60th vehicle measures the velocities and positions of its PVs (from the 1st to 59th vehicles), it can easily anticipate how the immediately preceding (59th) vehicle is going to behave (fluctuates its velocity) for $t > 100$ s. The 60th vehicle can avoid the harsh impact of the jamming wave by predicting its PVs and FVs and by taking appropriate control action a few seconds earlier. If a vehicle can reduce the usage of the accelerator and the brake, its fuel consumption, emission, and driving comfort will be improved and, consequently, the following traffic will benefit. With this motivation, the following section describes a smart-driving system using the MPC.

III. Smart-Driving System

The development of a smart-driving system in an MPC framework is described in this section. The MPC is only installed in a vehicle called the host vehicle, which computes its optimal control input by predicting the future trajectories of its PVs and FVs. Here, it is assumed that the other vehicles are driven according to the OVM by imitating human driving behavior. This implies that the OVM is used to predict the human-driven traffic in the MPC framework. It is also assumed that a local feedback control system that determines and applies the actual engine torque to realize the desired acceleration considering vehicle–engine dynamics is installed in the vehicle. The velocity of a vehicle is only determined by the state of its immediate PV, and the vehicles behind the host vehicle have no influence on its resulted velocity. However, to avoid any negative influence on the traffic behind the host vehicle, it is also necessary to consider the state of the FV in deciding the control action of the host vehicle. Therefore, the dynamics of a few PVs and an FV is included in designing a smart-driving system for the host vehicle. The control purpose is to only regulate the host vehicle by safely adjusting its headway in such a way that both the host and the FVs can flow without aggressive braking and large drops in their velocity. For simplicity, the host vehicle that is controlled by the smart-driving system is henceforth called the smart vehicle in this paper.

A. Problem Formulation

Fig. 2 shows an image of the smart-vehicle control problem considering its immediate FV F_1 and the N PVs $P_1, \ldots, P_N$ in the traffic. As shown by the blocks in the figure, the dynamics of the vehicles is described in two parts. The first part is the controlled plant for driving the smart vehicle, and the other part is for predicting the trajectories of the PVs.

In the smart-vehicle controller, the state vector consisting of the current position x_{f_1} and velocity v_{f_1} of the immediate FV, and the current position x_h and velocity v_h of the smart vehicle, which is denoted by $x = [x_{f1}, v_{f1}, x_h, v_h]^T$, is available. The control input of the smart vehicle u_h represents its acceleration, which is assumed to be bounded by the inequality constraint

$$-u_{\max} \le u_h \le u_{\max}. \tag{4}$$

The dynamics of the vehicles can be expressed as

$$\dot{x} = f_c(x, u_h) := \begin{bmatrix} v_{f_1} \\ g(x_{f_1}, x_h, v_{f_1}) \\ v_h \\ u_h \end{bmatrix} \tag{5}$$

where the acceleration function $g(\cdot,\cdot,\cdot)$ of the immediate FV is supposed to be given by the OVM in (1) as

$$g(x_{f_1}, x_h, v_{f_1}) = \kappa \left[V_{\rm op}(\Delta x_{f1}) - v_{f_1}\right]. \tag{6}$$

To keep the safe headway of the smart vehicle, it is necessary to consider the position of its immediate PV x_{p_1} in computing control input u_h. However, the trajectory of x_{p_1} can be only predicted if the dynamics of vehicles P_1–P_N is known, which is described in the following. The positions and velocities of these PVs are represented by vector $z = [x_{p_1},\, v_{p_1}, \ldots, x_{p_N}, v_{p_N}]$. We consider that their dynamics is given by the OVM, i.e.,

$$\dot{z} = f_p(z, r) := \begin{bmatrix} v_{p_1} \\ g(x_{p_1},\, x_{p_2}, v_{p_1}) \\ v_{p_2} \\ g(x_{p_2}, x_{p_3}, v_{p_2}) \\ \vdots \\ v_{p_{(N-1)}} \\ g\left(x_{p_{(N-1)}}, x_{p_N}, v_{p_{(N-1)}}\right) \\ v_{p_N} \\ a_{p_N} \end{bmatrix} \tag{7}$$

where parameter $r = a_{p_N}$ denotes the acceleration of the Nth PV. The value of a_{p_N} cannot be estimated using (6) since Δx_{p_N} is assumed to be unknown. Therefore, $a_{p_N}(t)$ is estimated at real time t, and for $\tau > t$, it is obtained as

$$\begin{aligned} a_{p_N}(\tau) &= f_{a_{p_N}}\left(v_{p_N}(\tau), a_{p_N}(t)\right) \\ &:= \frac{a_{p_N}(t)}{\left(1+e^{-\beta_1\left(v_{p_N}(\tau)-\gamma_1\right)}\right)\left(1+e^{\beta_2\left(v_{p_N}(\tau)-\gamma_2\right)}\right)} \end{aligned} \tag{8}$$

where the parameters γ_1 and γ_2 of the sigmoidal functions in (8) define an approximate range of velocities. Equation (8) states that $a_{p_N}(\tau) \approx a_{p_N}(t)$ if $v_{p_N}(\tau)$ is within that range from γ_1 to γ_2; otherwise, $a_{p_N}(\tau) \approx 0$, and β_1 and β_2 express the sharpness of the sigmoidal functions. This implies that the acceleration of the Nth PV approaches zero when the vehicle reaches a maximum velocity or completely stops, and the vehicle never moves backward.

For the implementation of the smart-driving system, it is necessary to measure the velocities and positions of the N PVs and the FV, and in addition, the acceleration of the Nth PV. Collecting information from the PVs at real time t is an important issue for realizing the proposed smart-driving system. It is assumed that the information from the sensory systems of the other vehicles is available precisely through V2V communications based on wireless technology with negligible delay. It is also assumed that the control input can be directly fed to the smart vehicle using an advanced ACC system that can operate in stop-and-go traffic without any response delay. Therefore, with the aforementioned technological and operational assumptions, it can be stated that the smart-driving system that is developed here is feasible.

B. MPC

In defining a cost function, it is also necessary to take into account the collision avoidance between the smart vehicle and its PV by assigning appropriate separation. A common way to define the desired headway $S_d(t)$ at time t with velocity $v_h(t)$ is

$$S_d(t) = S_0 + t_{\rm hd} v_h(t) \tag{9}$$

where S_0 is the minimum separation between the vehicles and $t_{\rm hd}$ is the time headway for safe car following. Time headway defines the number of seconds that is required by a vehicle to reach the current position of its PV. In this paper, the aforementioned preference of maintaining a velocity-dependent safe distance is taken into account in the form of a soft constraint, which is described in the setting of the performance index in the following.

The inequality constraint (4) that relates the amplitude of the control input is converted into an equivalent equality constraint by introducing a dummy input u_d as

$$C(x, u) := \left(u_h^2 + u_d^2 - u_{\max}^2\right) = 0 \tag{10}$$

where control vector u is defined as $u = [u_h,\, u_d]^T$. Subject to the dynamics of the vehicles [see (5)] and constraint (10), the optimal control problem, i.e.,

$$\min_u J := \min_u \int_t^{t+T} L\left(x(\tau), u(\tau), q(\tau)\right) d\tau \tag{11}$$

is solved for $u(t)$ at time t with the current state $x(t)$ used as the initial state, where $q = x_{p_1}$ is the time-varying parameter denoting the trajectory of the vehicle P_1, and T is the horizon over which the optimal control inputs are determined. The cost function, i.e.,

$$\begin{aligned} L(x, u, q) = {} & w_v \left(v_h(t) - V_d\right)^2 + w_u u_h^2(t) \\ & + w_f g^2\left(x_{f_1}(t), x_h(t), v_{f_1}(t)\right) \\ & + w_s(t) S_{\rm err}^2(t) \end{aligned} \tag{12}$$

is chosen in this paper to have four terms, where V_d is the desired velocity; w_v, w_u, and w_f are the constant weights; $S_{\rm err} \triangleq S_d - (x_{p_1} - x_h)$ is the separation error or the deviation from the desired headway; and $w_s(t)$ is the time-varying weight. The first term in (12) is used to represent the cost of the deviation of the smart vehicle from its desired velocity and the second term represents the cost of its acceleration. Minimizing these two cost terms leads to the steady driving of the smart vehicle. The third term represents the cost of acceleration in the FV. The last term is related to the aforementioned soft constraint for the safe driving of the smart vehicle and represents the cost that is due to a shorter distance of the smart vehicle than the desired one with respect to the immediate PV. Weighting function $w_s(t)$ provides a large penalty when it is very close to the PV and a negligible penalty when it is far away from the PV, which is defined as

$$w_s(t) = a_1 e^{-a_2 \tanh\left(a_3(t_h(t) - t_{\rm hd})\right)} \tag{13}$$

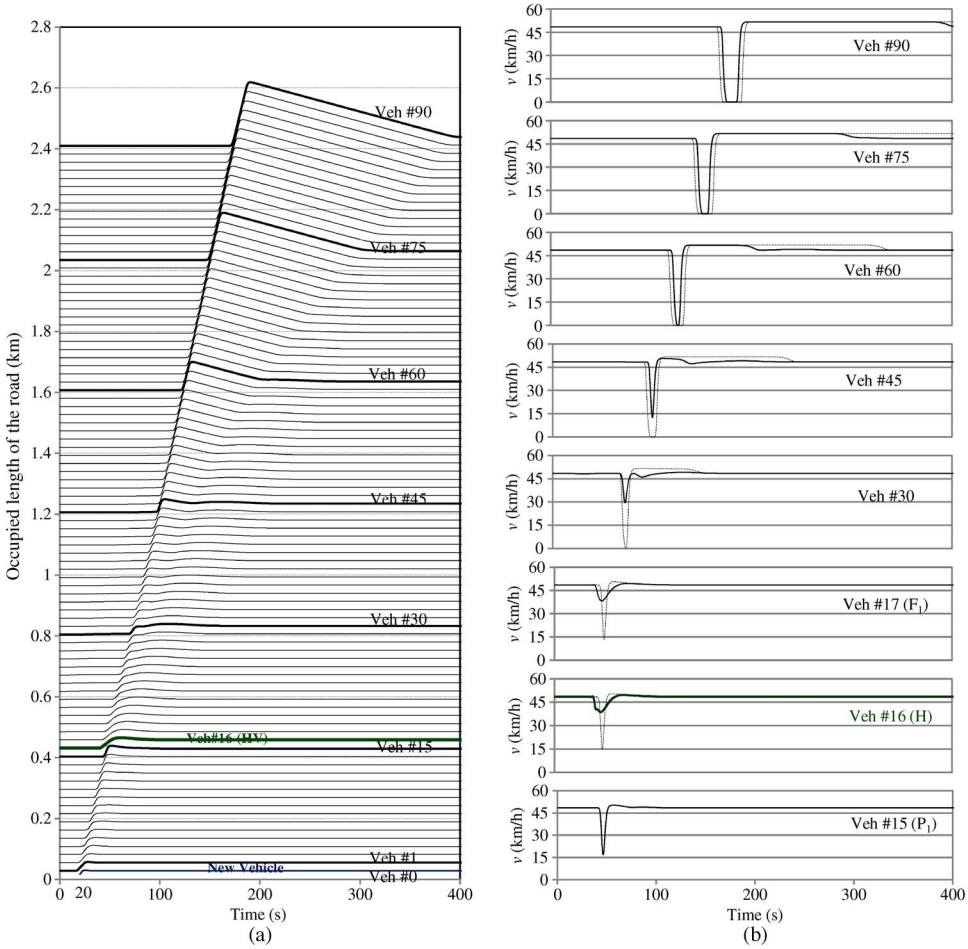

Fig. 3. Performance of the smart vehicle (the 16th vehicle) with $N = 4$ and its influence on the 17th to 90th vehicles in the following traffic. (a) Relative positions of the vehicles to Veh #0; the gap between two curves shows the corresponding separation of two vehicles. (b) Corresponding velocities (v, km/h) of selected vehicles; the thin dotted curves show the corresponding velocities found in Fig. 1.

where $t_h(t) = (x_{p1}(t) - x_h(t) - S_0)/(v_h(t) + \alpha)$ is the time-headway, where a small constant α is added to avoid singularity at $v_h = 0$.

In the implementation of the MPC with a given horizon, the optimal control problem formulated earlier is discretized. At each discrete time step, the control inputs u_h of the smart vehicle for the entire horizon are computed by solving the optimal control problem that is expressed by the given dynamics, the constraint, and the performance index. However, only the immediate control input is applied to drive the smart vehicle. The whole process is repeated throughout the driving course. Repeating the whole process and renewing the control input at each sampling time are necessary to overcome the influences of varying traffic and unmodeled disturbances in reality. In this paper, the continuation and generalized minimum residual (C/GMRES) method is used to compute the solution of the given predictive vehicle control problem [22]. Since the C/GMRES method does not require iterative searches, it is much faster than any other iterative method. The work in [23] has shown that the computation time of the C/GMRES method for solving an optimal vehicle control problem is less than 10 ms; therefore, this method is very suitable for a real-time vehicle control system. A brief overview of the implementation approach of the proposed MPC is described in the Appendix.

IV. Numerical Simulation

The numerical simulation of the proposed vehicle driving system has been conducted by choosing an arbitrary vehicle as the smart vehicle from the traffic. The purposes of simulation are to evaluate the following aspects: 1) the improvement in the driving behavior of both the smart vehicle and the FVs; 2) the attenuation of jamming waves from the following traffic; 3) the prediction accuracy and performance with respect to the number of PVs considered in the smart-driving system; and 4) the justification of including the dynamics of the FV in determining the control input of the smart vehicle. The driving and controlling preferences are set as $u_{\max} = 3.75$ m/s^2, $t_{\rm hd} = 1.8$ s, $V_d = 16.67$ m/s, $w_v = 0.6$, $w_u = 10$, and $w_f = 30$. The weighting parameters of w_s that are given by (13) is set at $\alpha = 0.1$, $a_1 = 0.03$, $a_2 = 8.88$, and $a_3 = 0.27$. The prediction function (8) for the acceleration of the Nth PV is set with $\beta_1 = 5.0$, $\beta_2 = 1.0$, $\gamma_1 = 0.50$, and $\gamma_2 = 13.0$. The simulation time step and the prediction horizon are set at $\Delta\tau = 0.05$ s and $T = 20$ s, respectively.

The proposed smart-driving system is evaluated in this section for the traffic-flow conditions illustrated in Fig. 1. Specifically, all vehicles flow in the same way according to the OVM, except the 16th vehicle. The 16th vehicle is selected as the smart vehicle and is driven by using the proposed control system

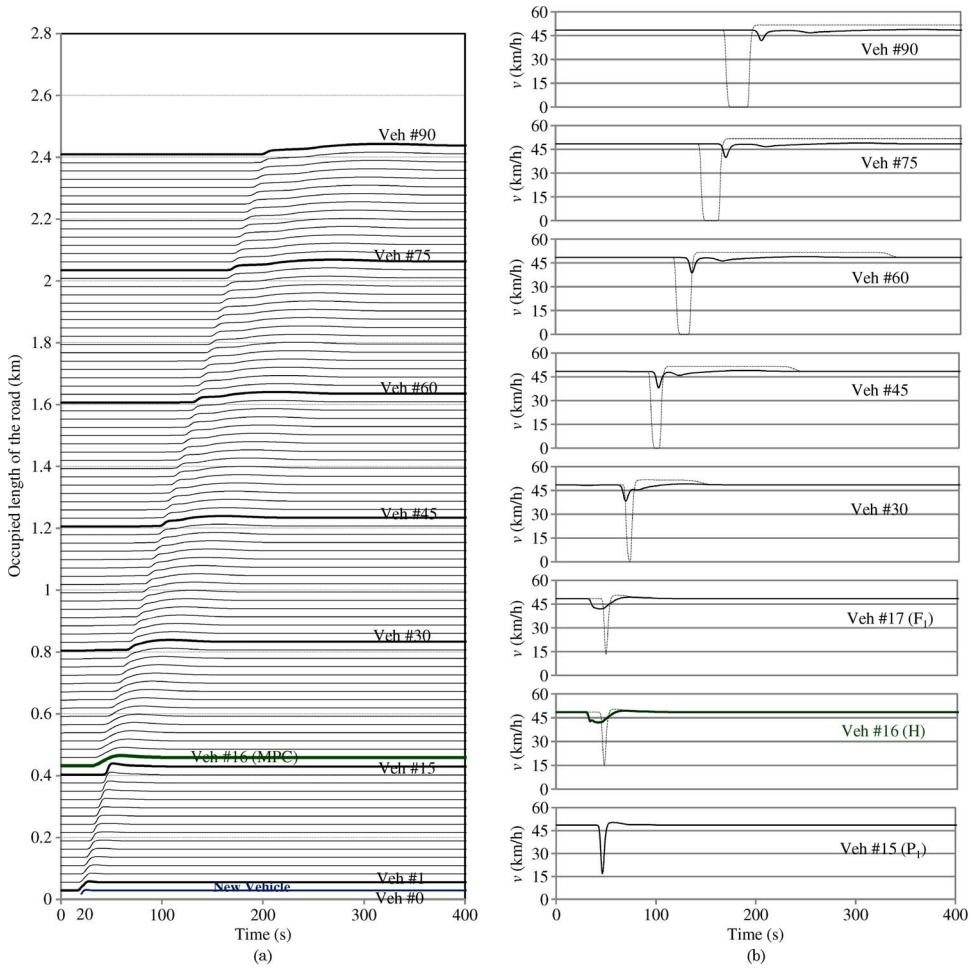

Fig. 4. Performance of the smart vehicle (the 16th vehicle) with $N = 8$ and its influence on the 17th to 90th vehicles in the following traffic. (a) Relative positions of the vehicles to Veh #0; the gap between two curves shows the corresponding separation of two vehicles. (b) Corresponding velocities (v, km/h) of selected vehicles; the thin dotted curves show the corresponding velocities found in Fig. 1.

from the beginning. At first, the smart vehicle is controlled by predicting its $N = 4$ PVs. Fig. 3(a) shows the relative positions of the vehicles in the traffic. As soon as the system recognizes deceleration in vehicle P_4 (Veh#12), by predicting the states of its PV P_1 (Veh#15), it immediately starts adjusting the velocity of the smart vehicle and increases the headway before facing the jamming wave. Fig. 3(b) shows the corresponding velocities of selected vehicles in the traffic. The dotted curves in the velocity graphs show the corresponding values previously observed without employing the proposed control system in any vehicle. The smart vehicle (Veh#16) starts dropping its velocity a little earlier than the PV (Veh#15). Therefore, in this way, it avoids an abrupt change in velocity due to the jamming wave that is caused by the appearance of a new vehicle in the preceding traffic. Consequently, the flow of its FV (Veh#17) also improves significantly. It seems that the reduction of fluctuation is not enough to keep the following traffic in the string-stable region. Although the proposed control of the smart vehicle fails to completely eliminate the jamming wave, it delays the propagation of the jamming wave and some of the FVs benefit from it.

The performance of the system can be further improved if more vehicles are used in the model to predict the jamming waves in the preceding traffic. Fig. 4 shows the results that correspond to the case of $N = 8$ PVs. In this case, the system recognizes any changes in the P_8 vehicle (Veh#8) and predicts its consequences earlier than the case of $N = 4$. Early recognition of a jamming wave enables the smart vehicle to take more cautious action in advance. In this case, the jamming wave is almost eliminated from the following traffic, as shown in Fig. 4. This implies that the FVs remain in the string-stable region. The results justify that the larger the value of N is, the better accuracy in the prediction of the jamming wave is realized.

In the smart-driving system, although there is no control over the FV, its dynamics is also included in the vehicle control framework and the performance index includes a cost term that corresponds to the acceleration of the FV with weight w_f. The results shown in Figs. 3 and 4 correspond to $w_f = 30$. The necessity of considering the FVs in determining the control input of the smart vehicle is also investigated here. For the case with $N = 8$, the performance of the smart vehicle is evaluated by ignoring the cost of acceleration of the FV in the performance index by setting $w_f = 0$. Fig. 5 shows the velocities of those vehicles in the traffic. The curves "WithFV" and "WithoutFV" represent the velocities that correspond to the cases with $w_f = 30$ and $w_f = 0$, respectively. In the case of $w_f = 0$, only the minimization of the acceleration of the smart vehicle is considered, and this results in very little improvement

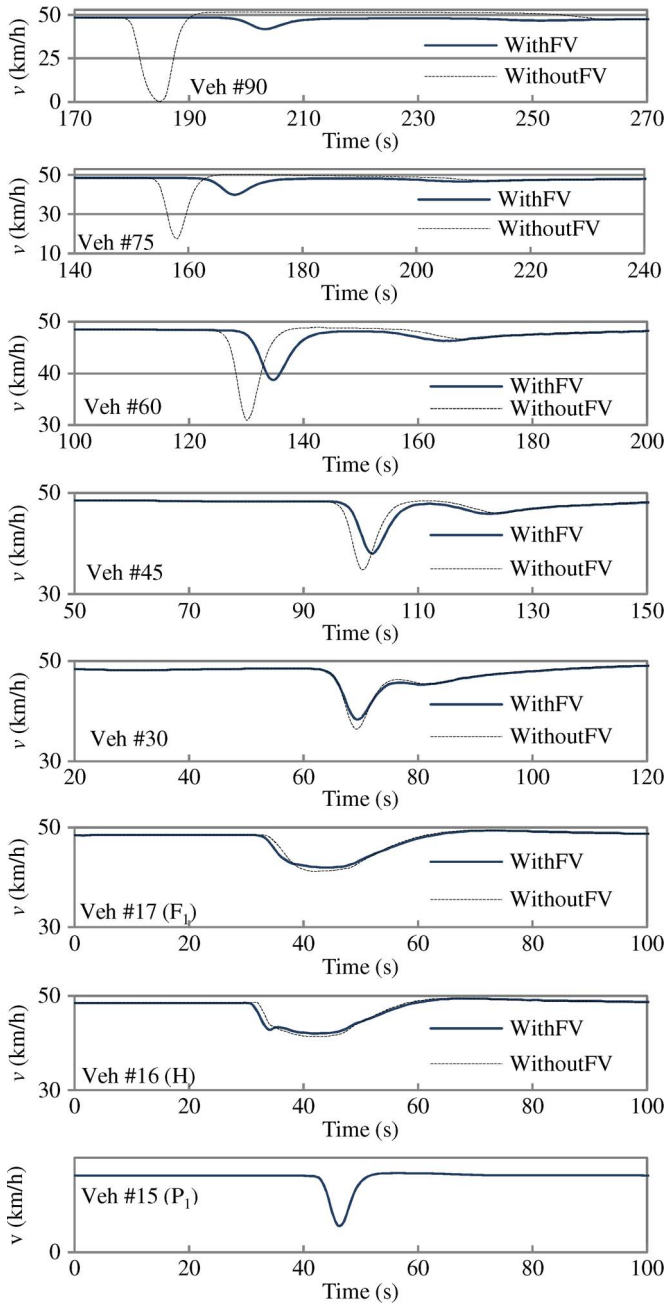

Fig. 5. Velocities of selected vehicles in the traffic. The curves WithFV and WithoutFV represent the velocities that correspond to the cases with $w_f = 30$ and $w_f = 0$, respectively.

of its velocity compared with the case of $w_f = 30$. However, it slightly increases the velocity deviation in the FV. This deviation later propagates in the following traffic and the jamming wave evolves. In other words, the marginal role WithFV could pull back the local traffic into a stable region that eventually attenuates the waves. The results justify the proposed vehicle driving system that also considers the dynamics of the FV to improve the flow of the following traffic.

The proposed method is finally tested in a worse traffic-flow condition, in which density waves continuously propagate. The evolution of such periodical congestion is realized through a periodical perturbation in the first vehicle, which is similar to the numerical simulation in [21]. Fig. 6 shows the relative positions of vehicles in the traffic for the case of $w_f = 30$ and $w_f = 0$. Initially, all vehicles run according to the OVM. In this observation, parameters V_1 and V_2 are set at 8.0 and 8.67, respectively [20]. In period $t < 200$, the jamming waves evolve in the traffic due to the continuous periodical fluctuations in the first vehicle. Due to the jamming waves, these vehicles occupy about 2.47 km of the road, which corresponds to an average density of 36.4 veh/km. At $t = 200$ s only the 40th vehicle, which is chosen as the smart vehicle, is switched on to be driven by the proposed smart-driving system. Although its preceding traffic continuously oscillates, the smart vehicle attenuates the jamming waves mostly and keeps the velocity steadier than the preceding traffic, as shown in Fig. 6(a). By its influence, in a similar fashion, the flow of all following traffic is also improved and all these vehicles require a space of 2.25 km on the road, which corresponds to the average density of 40.0 veh/km. On the other hand, Fig. 6(b) shows the case that controls the smart vehicle by ignoring the FV with $w_f = 0$. In this case, the jamming waves are only partially attenuated and these vehicles require a space of 2.38 km on the road, which corresponds to an average density of 37.8 veh/km. These results justify the necessity of considering the FV in controlling the smart vehicle.

V. Discussion

A smart-driving system has been developed to control only a single vehicle and it is evaluated in dense human-driven vehicular traffic containing jamming waves. The smart vehicle can perform well only when there is some freedom in adjusting its velocity, i.e., the traffic is dense but not fully congested. If the amplitude and duration of the jamming waves are large, the smart vehicle may be able to only attenuate them partially and they may evolve and propagate backward later. Multiple smart vehicles can be easily connected for cooperative driving and may eliminate jamming waves from the traffic more efficiently. Such an intensive study of multiple smart vehicles or a platoon is kept for future work. The proposed system is effective in attenuating any jamming wave at its initial stage or at least delay the occurrence of a shock wave and traffic breakdown.

Various traffic-flow models that represent human driving behavior have been studied in road transportation research. Each model has its merits and limitations. In this paper, we have used the OVM for a traffic-flow model as it simply describes traffic dynamics using a differential equation. The OVM describes various properties of traffic congestion, such as the fundamental diagram, the formation of shock waves, and traffic breakdown. As an example in this paper, the OVM is used to create virtual traffic to evaluate the performance of a vehicle with the proposed smart-driving system.

In reality, the actual car-following behavior is neither identical among vehicles nor known in advance by a controller. In this paper, as the first step of this development, the OVM with the same parameters for all the vehicles is used to predict the future behavior of every vehicle in the MPC framework and the smart-driving system is evaluated in the traffic containing vehicles with identical behavior. However, in the proposed framework, the behavior of vehicles that is predicted by $g(\cdot)$ in

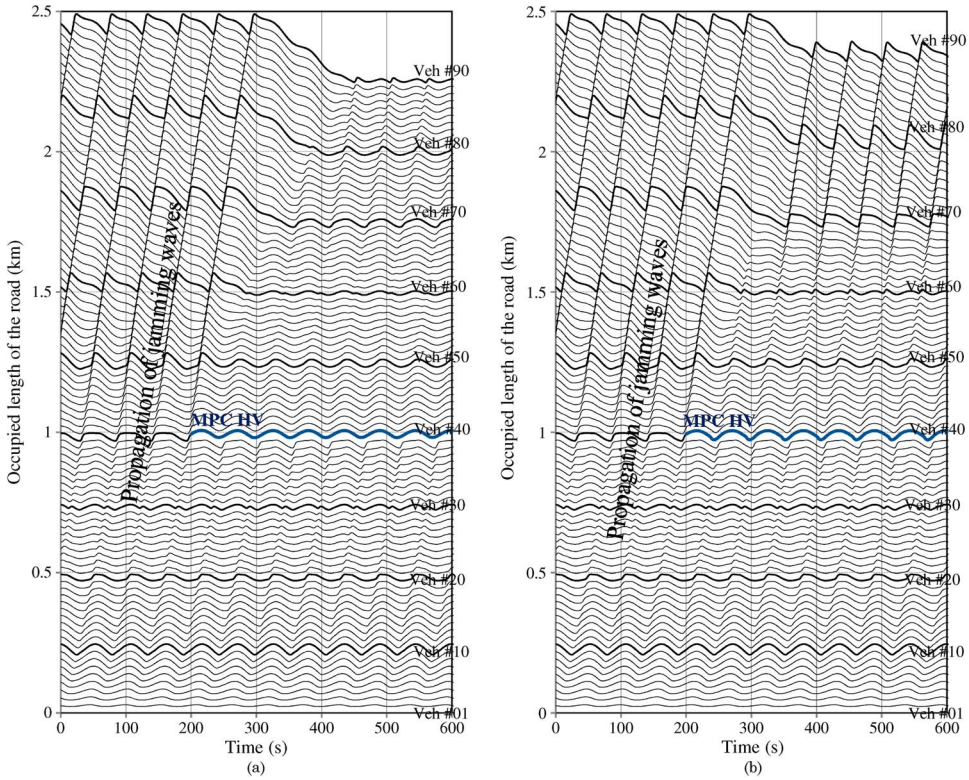

Fig. 6. Distribution of vehicles on the road. Propagation of jamming waves whose magnitudes are attenuated by the 40th vehicle driven by the proposed control system for $t > 200$. (a) Case $w_f = 30$. (b) Case $w_f = 0$.

(5), (6), and (7) can be flexibly replaced according to a supposed situation to be considered. In future work, the following two issues should be investigated before implementing the proposed smart-driving system: 1) the robustness of the smart-driving system against the diversity of behavior among vehicles in nonuniform traffic while using the same OVM in the MPC framework and 2) the possibility of performance improvement using the nonuniform OVM according to the behavior of individual vehicles in nonuniform traffic.

The framework includes the FV, along with a few PVs in the decision process. The inclusion of an FV or an additional PV may play a role in slightly attenuating any disturbance in the nearby traffic. Sometimes, such slight local improvement is sufficient to pull back the traffic into the stable region. However, the inclusion of the FV in the framework is more significant. It implies that the vehicle should not be braked hard in any circumstance that may cause rear-end collision with the FV. For example, a vehicle may need to change its velocity for some other reasons, e.g., for a stop on the roadside or turning at the intersection. Considering the FV in the control framework, the host vehicle can regulate its braking/deceleration rates without affecting the following traffic in such cases.

The proposed smart-driving system differs from the conventional ACC or CACC in terms of its action-taking mechanism. The ACC or the CACC takes a control decision based on the actual condition (acceleration, velocity, and position) of the PV. Therefore, if there is sudden acceleration in the PV, counter action can be only taken after detecting it. On the other hand, the smart-driving system predicts the acceleration of the PV before it happens by detecting and analyzing multiple vehicles in the preceding traffic.

Conventional sensing technology, such as an onboard camera, a laser, or other sensors, has limitations in precise detection and measurement of the state of vehicles beyond its immediate PV. V2V communication may provide the information of surrounding vehicles with high accuracy in a connected vehicles environment. Since V2V communication is an emerging technology that is currently under experimentation in intelligent transportation systems, the details of this technology are not addressed in this paper.

VI. Conclusion and Future Work

A smart-driving system for a vehicle using the MPC has been proposed. By predicting any jamming wave in the preceding traffic, the optimal control input is determined through rigorous computation aiming at the smooth driving of a smart vehicle and minimizing the adverse effects on the human-driven FV while regulating a safe headway from the PV. The proposed system has been evaluated by numerical simulation in dense traffic that contains jamming waves. It is observed that the system alleviates congestion-forming phenomena from the traffic and improves the traffic flow by only controlling a single vehicle. Since the smart vehicle significantly attenuates the jamming waves, the flow of vehicles in the following traffic becomes smooth. Such smart driving of vehicles is believed to be very conducive in improving traffic flow, driving comfort, and energy consumption and emissions, and is thereby useful in developing sustainable road transportation systems.

It will be also one of our future works to enhance the proposed smart-driving system for the cooperative driving of multiple vehicles or a vehicle platoon for further improvement of traffic flow.

APPENDIX
IMPLEMENTATION OF MPC

The implementation of the proposed MPC for vehicle driving requires fast computation to solve the optimal control problem. The C/GMRES method solves a nonlinear MPC problem very quickly since it does not require any iterative search. A brief overview of the method that is used to solve the MPC problem is described in this section. The details of the C/GMRES method, its error analysis, and the proof of the algorithm are described in the work in [22].

The Hamiltonian function is formed using (5), (10), and (12), as

$$H(x,\lambda,u,\psi,q) := L(x,u,q) + \lambda^T f(x,u) + \psi^T C(x,u) \tag{14}$$

where vector λ denotes the costate and ψ denotes the Lagrange multiplier that is associated with the constraint.

To numerically solve the optimal control problem, horizon T is discretized into M steps of size $\Delta\tau = T/M$. The necessary conditions of the optimality are obtained in the form

$$\begin{aligned} &F\left(Y(t),x(t),t\right) \\ &:= \begin{bmatrix} H_u^T\left(x_0^*(t),\lambda_1^*(t),u_0^*(t),\psi_0^*(t),q_0^*(t)\right) \\ C\left(x_0^*(t),u_0^*(t)\right) \\ \vdots \\ H_u^T\left(x_{M-1}^*(t),\lambda_M^*(t),u_{M-1}^*(t),\psi_{M-1}^*(t),q_{M-1}^*(t)\right) \\ C\left(x_{M-1}^*(t),u_M^*(t)\right) \end{bmatrix} \\ &= 0 \end{aligned} \tag{15}$$

where H_u is the Jacobian; $\{x_i^*(t)\}_{i=0}^{M-1}$, $\{\lambda_i^*(t)\}_{i=1}^{M}$, $\{u_i^*(t)\}_{i=0}^{M-1}$, $\{\psi_i^*(t)\}_{i=0}^{M-1}$, and $\{q_i^*(t)\}_{i=0}^{M-1}$ denote the corresponding discretized values; and

$$Y(t) := \left[u_0^{*T}(t),\psi_0^{*T}(t),\ldots,u_{M-1}^{*T}(t),\psi_{M-1}^{*T}(t)\right]^T. \tag{16}$$

At first, time-varying parameter $q(t) = x_{p_1}(t)$ is estimated with the given states of PVs $P_1,\ldots,P_N$ using (7) and (8) as

$$z_0^*(t) = z(t) \tag{17}$$

$$r_0^*(t) = a_{p_N}(t) \tag{18}$$

$$z_{i+1}^*(t) = z_i^*(t) + f_p\left(z_i^*(t),u_i^*(t),r_i^*(t)\right)\Delta\tau \tag{19}$$

$$r_{i+1}^*(t) = f_{a_{p_N}}\left(v_{p_N i}^*(t),a_{p_N}(t)\right) \tag{20}$$

$$q_i^*(t) = x_{p1i}^*(t). \tag{21}$$

Next, with a given vector $Y(t)$, the discretized sequences of the states are obtained as

$$x_0^*(t) = x(t) \tag{22}$$

$$x_{i+1}^*(t) = x_i^*(t) + f_c\left(x_i^*(t),u_i^*(t)\right)\Delta\tau. \tag{23}$$

The sequence of the costate is recursively determined using Jacobian H_x and the terminal costate $\lambda_M^*(t) = 0$ as

$$\lambda_i^*(t) = \lambda_{i+1}^*(t), + H_x^T\left(x_i^*(t),\lambda_{i+1}^*(t),u_i^*(t)\psi_i^*(t),q_i^*(t)\right)\Delta\tau.$$

In determining the optimal control input over the horizon, nonlinear equation (15) needs to be solved with a given $Y(t)$ and $x(t)$ at each time t. Instead of a costly iterative algorithm, the solution of the aforementioned optimal control problem is efficiently traced out by using the C/GMRES method [22]. It is based on the idea that F can identically be zero if

$$\frac{d}{dt}F\left(Y(t),x(t),t\right) = -\zeta F\left(Y(t),x(t),t\right) \tag{24}$$

$$F\left(Y(0),\,x(0),\,0\right) = 0 \tag{25}$$

where ζ is a positive constant to stabilize $F = 0$. Condition (24) can be rewritten as a linear equation for $\dot{Y}$ using Jacobian matrices F_Y, F_x, and F_t as

$$F_Y\dot{Y} = -F_x\dot{x} - F_t - \zeta F. \tag{26}$$

This can be efficiently solved by a linear solver, i.e., the GMRES, and solution $Y(t)$ is updated by integrating $\dot{Y}$ in real time using the continuation method [22], [24]. In the C/GMRES method, the set of control inputs is used as the initial guess of the solution of the optimization problem for the next sampling step with newly measured states. Since this method is much faster than any iterative method, it can be implemented for an onboard vehicle control system in real time.

ACKNOWLEDGMENT

The authors would like to thank T. Kawabe from Kyushu University, Fukuoka, Japan, for giving the inspiring idea of vehicle control for improving traffic flow.

REFERENCES

[1] T. Nagatani, "The physics of traffic jams," *Rep. Prog. Phys.*, vol. 65, no. 9, pp. 1331–1386, Sep. 2002.
[2] D. Helbing, "Traffic and related self-driven many-particle systems," *Rev. Mod. Phys.*, vol. 73, no. 4, pp. 1067–1141, Oct.-Dec. 2001.
[3] Y. Sugiyama, M. Fukui, M. Kikuchi, K. Hasebe, A. Nakayama, K. Nishinari, S. Tadaki, and S. Yukawa, "Traffic jams without bottlenecks—Experimental evidence for the physical mechanism of the formation of a jam," *New J. Phys.*, vol. 10, p. 033001, Mar. 2008.
[4] M. R. Flynn, A. R. Kasimov, J. C. Nave, R. R. Rosales, and B. Seibold, "Self-sustained nonlinear waves in traffic flow," *Phys. Rev. Part E*, vol. 79, no. 5, pp. 056113-1–056113-13, 2009.
[5] C. C. Chien, Y. Zhang, and P. A. Ioannou, "Traffic density control for automated highway systems," *Automatica*, vol. 33, no. 7, pp. 1273–1285, Jul. 1997.
[6] A. Hegyi, B. De Schutter, and J. Hellendoorn, "Optimal coordination of variable speed limits to suppress shock waves," *IEEE Trans. Intell. Transp. Syst.*, vol. 6, no. 1, pp. 102–112, Mar. 2005.
[7] A. Vahidi and A. Eskandarian, "Research advances in intelligent collision avoidance and adaptive cruise control," *IEEE Trans. Intell. Transp. Syst.*, vol. 4, no. 3, pp. 143–153, Sep. 2003.
[8] A. Kesting, M. Treiber, M. Schonhof, and D. Helbing, "Adaptive cruise control design for active congestion avoidance," *Transp. Res. Part C*, vol. 16, no. 6, pp. 668–683, Dec. 2008.
[9] M. Green, "How long does it take to stop? Methodological analysis of driver perception-brake times," *Transp. Human Factors*, vol. 2, no. 3, pp. 195–216, 2000.
[10] J. Ploeg, A. F. A. Serrarens, and G. J. Heijenk, "Connect & Drive: Design and evaluation of cooperative adaptive cruise control for congestion reduction," *J. Modern Transp.*, vol. 19, no. 3, pp. 207–213, 2011.
[11] B. V. Arem, J. G. Driel, and R. Visser, "The impact of cooperative adaptive cruise control on traffic-flow characteristics," *IEEE Trans. Intell. Transp. Syst.*, vol. 7, no. 4, pp. 429–436, Dec. 2006.
[12] Connected Vehicle Research, May 24, 2011. [Online]. Available: http://www.its.dot.gov/connected_vehicle/connected_vehicle.htm

[13] A. Kesting, M. Treiber, and D. Helbing, "Connectivity statistics of store-and-forward intervehicle communication," *IEEE Trans. Intell. Transp. Syst.*, vol. 11, no. 1, pp. 171–181, Mar. 2010.
[14] M. A. S. Kamal, J. Imura, A. Ohata, T. Hayakawa, and K. Aihara, "Efficient control of vehicle in congested traffic using MPC," in *Proc. IEEE Multi-Conf. Syst. Control*, 2012, pp. 1522–1527.
[15] M. Bando, K. Hasebe, A. Nakayama, A. Shibata, and Y. Sugiyama, "Dynamic model of traffic congestion and numerical simulation," *Phys. Rev. E*, vol. 51, pp. 1034–1042, 1995.
[16] M. Brackstone and M. McDonald, "Car-following: A historical review," *Transp. Res. Part F: Traffic Psych. Behaviour*, vol. 2, no. 4, pp. 181–196, 1999.
[17] K. Koshini, H. Kokame, and K. Hirata, "Decentralized delayed-feedback control of an optimal velocity traffic model," *Eur. Phys. J. B*, vol. 15, no. 4, pp. 715–722, Jun. 2000.
[18] D. Helbing and B. Tilch, "Generalized force model of traffic dynamics," *Phys. Rev. E*, vol. 58, no. 1, pp. 133–138, Jul. 1998.
[19] S. Tadaki, M. Kikuchi, Y. Sugiyama, and S. Yukawa, "Noise induced congested traffic flow in coupled map optimal velocity model," *J. Phys. Soc. Jpn.*, vol. 68, no. 9, pp. 3110–3114, 1999.
[20] W. Lv, W. Song, and Z. Fang, "Three-lane changing behavior simulation using a modified optimal velocity model," *Physica A*, vol. 390, no. 12, pp. 2303–2314, Jun. 2011.
[21] M. Herrmann and B. S. Kerner, "Local cluster effect in different flow models," *Physica A*, vol. 255, no. 1/2, pp. 163–188, Jun. 1998.
[22] T. Ohtsuka, "A continuation/GMRES method for fast computation of nonlinear receding horizon control," *Automatica*, vol. 40, no. 4, pp. 563–574, Apr. 2004.
[23] M. A. S. Kamal, M. Mukai, J. Murata, and T. Kawabe, "Model predictive control of vehicles on urban roads for improved fuel economy," *IEEE Trans. Control Syst. Technol.*, vol. 21, no. 3, pp. 831–841, May 2013.
[24] C. T. Kelley, *Iterative Methods for Linear and Nonlinear Equations*. Philadelphia, PA: SIAM, 1995, ser. In Frontiers in applied mathematics.

Md. Abdus Samad Kamal (S'01–M'07) received the B.Sc.Eng. degree from Khulna University of Engineering and Technology, Khulna, Bangladesh, in 1997 and the Master's and Ph.D. degrees from Kyushu University, Fukuoka, Japan, in 2003 and 2006, respectively.

He was a Lecturer with Khulna University of Engineering and Technology until 2000. He also served as a Post Doctoral Fellow with Kyushu University; as an Assistant Professor with International Islamic University Malaysia, Selayang, Malaysia; and as a Researcher with the Fukuoka Industry, Science, and Technology Foundation. He is currently with the Institute of Industrial Science, The University of Tokyo, Tokyo, Japan, and also with the Japan Science and Technology Agency, Kawaguchi, Japan, where he is a Researcher. His research interests include intelligent transportation systems and the applications of model predictive control.

Dr. Kamal is a member of the Society of Instrument and Control Engineers.

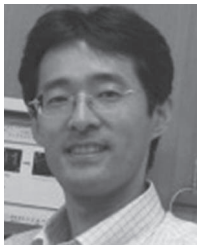

Jun-ichi Imura (M'93) received the M.S. degree in applied systems science and the Ph.D. degree in mechanical engineering from Kyoto University, Kyoto, Japan, in 1990 and 1995, respectively.

From 1992 to 1996, he was a Research Associate with the Department of Mechanical Engineering and Science, Graduate School of Engineering, Kyoto University and from 1996 to 2001, he was an Associate Professor with the Division of Machine Design Engineering, Faculty of Engineering, Hiroshima University, Hiroshima, Japan. From May 1998 to April 1999, he was a Visiting Researcher with Department of Applied Mathematics, University of Twente, The Netherlands. Since 2001, he has been with the Department of Mechanical and Environmental Informatics, Graduate School of Information Science and Engineering, Tokyo Institute of Technology, Tokyo, Japan, where he is currently a Professor. His research interests include analysis and control synthesis of nonlinear systems, hybrid systems, and large-scale complex dynamical networks, with applications to biological systems and industrial process systems.

He is an Associate Editor of IEEE TRANSACTIONS ON AUTOMATIC CONTROL, AUTOMATICA, AND NONLINEAR ANALYSIS: HYBRID SYSTEMS.

Tomohisa Hayakawa (S'00–M'04) received the B.Eng. degree in aeronautical engineering from Kyoto University, Kyoto, Japan, in 1997; the M.S. degree in aerospace engineering from The State University of New York, Buffalo, NY, USA, in 1999; and the M.S. degree in applied mathematics and the Ph.D. degree in aerospace engineering from Georgia Institute of Technology, Atlanta, GA, USA, in 2001 and 2003, respectively.

He was a Research Fellow with the Department of Aeronautics and Astronautics, Graduate School of Engineering, Kyoto University and with the Japan Science and Technology Agency in 2006, and then joined the Department of Mechanical and Environmental Informatics, Graduate School of Information Science and Engineering, Tokyo Institute of Technology, Tokyo, Japan, where he is currently an Associate Professor. His research interests include stability of nonlinear systems; nonnegative and compartmental systems; hybrid systems; nonlinear adaptive control; neural networks and intelligent control; stochastic dynamical systems; and applications to aerospace vehicles, formation control of multiagent systems, robotic systems, financial dynamics, and biological/biomedical systems.

Akira Ohata received the degree from Tokyo Institute of Technology, Tokyo, Japan, in 1973.

After graduating, he directly joined Toyota Motor Corporation, where he was involved in exhaust gas emission controls; intake and exhaust system developments, including variable intake systems, hybrid vehicle control system, vehicle controls, and model-based development; and the education of advanced control theory. He is currently a Senior General Manager with Toyota Motor Corporation, Shizuoka, Japan, and a Research Fellow with the Information Technology Promotion Agency (IPA), Tokyo, Japan, under the Ministry of Economy, Trade, and Industry. His research interests include modeling that includes model simplification and the integration of physical and empirical models.

Mr. Ohata is a Vice Chair of the International Federation of Automatic Control TC7.1 (automotive control) and the Chair of the Technical Committee on Plant Modeling of the Society of Instrument and Control Engineers. He oversees the standardization activity in Object Management Group, assuring the dependability of consumer devices. He received the Most Outstanding Paper Award in Convergence 2004 and the Technical Contribution Award from Japan Society of Automotive Engineers.

Kazuyuki Aihara received the B.E. degree in electrical engineering and the Ph.D. degree in electronic engineering from The University of Tokyo, Tokyo, Japan, in 1977 and 1982, respectively.

He is a Professor with the Institute of Industrial Science and with the Graduate School of Information Science and Technology, The University of Tokyo. He is also the Director of the Collaborative Research Center for Innovative Mathematical Modelling, Institute of Industrial Science, The University of Tokyo. His research interests include the mathematical modeling of complex systems, parallel distributed processing with spatiotemporal chaos, and the time-series analysis of complex data.